Laboratory activity 0: Position PID–control of a DC servomotor

(Theoretical background)

Riccardo Antonello* Francesco Ticozzi*

March 19, 2025

1 Activity goal

The goal of this laboratory activity is to design a PID position controller for the DC servomotor available in the laboratory. The design is carried out in the frequency domain (i.e., using the *Bode's method*) with the adoption of a nominal model of the motor, whose parameters are deduced from the datasheets. In the second part of the activity, the motor parameters, including static and viscous friction, are estimated through simple experimental tests. These parameters will be used in the next laboratory activity to improve control performance, particularly by implementing a feedforward inertia and friction compensation scheme.

2 Analytical model of the DC gearmotor

The electromechanical structure of a permanent-magnet DC motor is shown in Fig. 1. A rotation of the motor shaft is obtained as the result of the interaction of the magnetic field generated by the armature current with the existing field produced by the stator magnets. A device called *commutator* is used to keep the armature current flowing always in the same direction within the stator field; maximum torque is achieved by always supplying the armature current to the armature coil faced

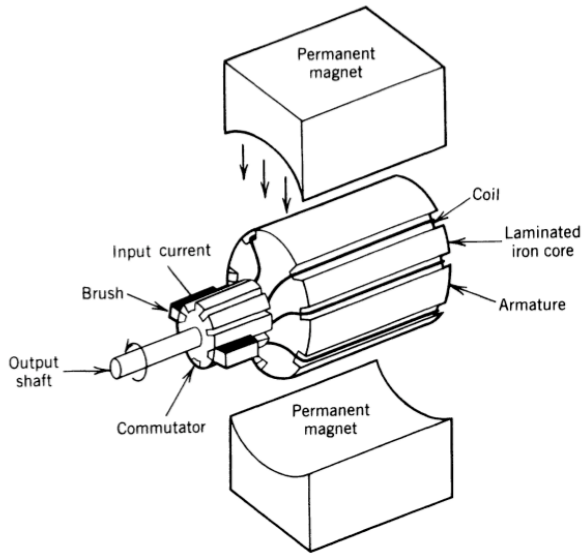

Figure 1: Electromechanical structure of a permanent–magnet DC motor.

*Dept. of Information Engineering (DEI), University of Padova; email: {antonello, ticozzi}@dei.unipd.it

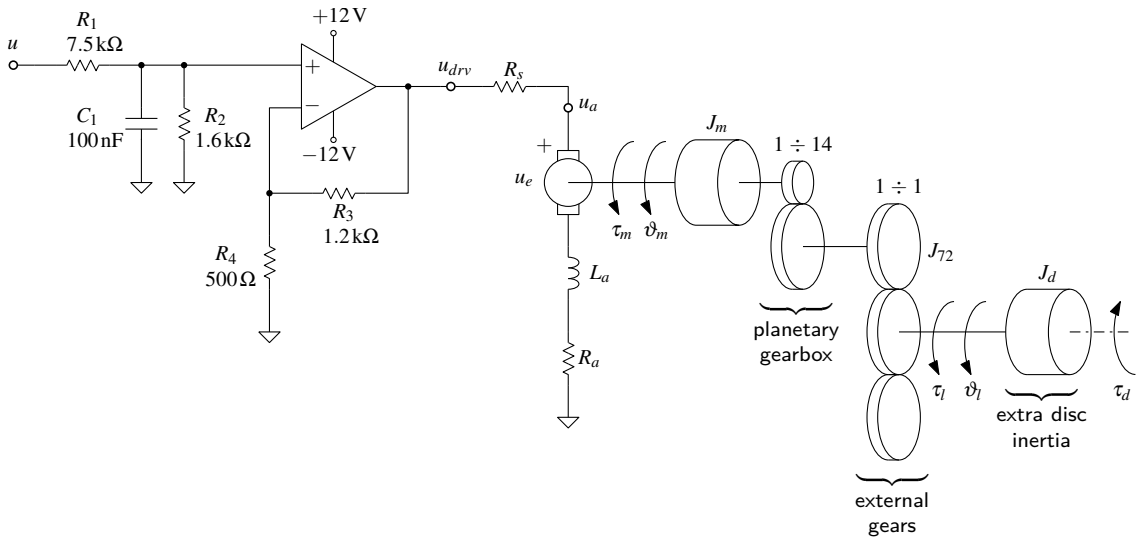

Figure 2: DC gearmotor: lumped–element diagram.

perpendicularly to the stator field. Electrical contacts called *brushes* (typically, spring-loaded carbon contacts) are used to supply the electric current to the commutator and, in turn, the armature coils.

The lumped-element diagram of the Quanser SRV–02 gearmotor available in laboratory is shown in Fig. 2. In the diagram, the DC motor is represented by the equivalent electric circuit of its armature (i.e. series connection of the resistance R_a, inductance L_a, and back electromotive force source u_e), and the rotor moment of inertia J_m. The rotor inertia is moved by the motor torque τ_m, which originates from the interaction of the magnetic fields generated by the armature current and the stator permanent magnets. A gearbox is used to transfer the rotary motion to an external *inertial load* with moment of inertia J_d. The connection between the gearbox and the mechanical load is assumed to be rigid (i.e. no elasticity is present in between the two elements). The armature voltage u_a is supplied by a voltage driver. A shunt resistor R_s is connected in between the voltage driver output and the armature circuit. By sensing the voltage drop across such resistor (i.e. the difference between the driver output voltage u_{drv} and the armature voltage u_a), and knowing the nominal value of the resistor, it is possible to infer the current passing through the resistor, which is indeed the armature current i_a. A complete definition of the symbols used in Fig. 2 is reported in Tab. 1.

J_m, B_m	rotor moment of inertia and viscous friction coefficient
J_l, B_l	load moment of inertia and viscous friction coefficient
R_a, L_a	resistance and inductance of the armature circuit
u_a, i_a	supply voltage and current to the armature circuit
u_e	back electromotive force (BEMF)
k_t, k_e	torque and electric (BEMF) constants
τ_m, ω_m, ϑ_m	*motor side* torque, speed and position
τ_l, ω_l, ϑ_l	*load side* torque, speed and position
τ_d	disturbance torque applied to the load inertia
N	planetary gearbox reduction ratio
R_s	shunt resistance
u, u_{drv}	voltage driver input and output voltages
k_{drv}, $f_{c,drv}$	voltage driver attenuation gain and cut–off frequency

Table 1: DC gearmotor with inertial load: symbols definitions.

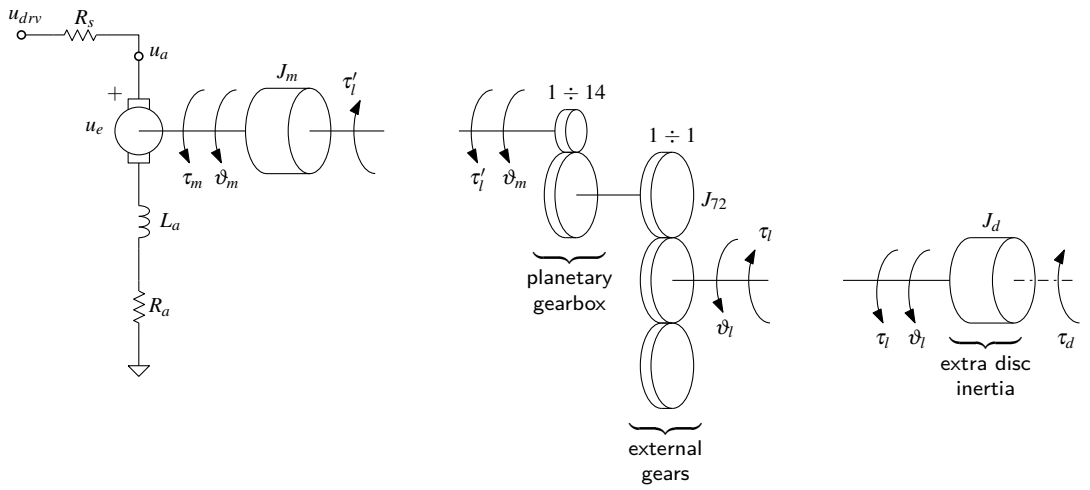

Figure 3: DC gearmotor: free–body diagram.

Regarding the load inertia J_l, this is equal to $J_l = J_d + 3\,J_{72}$, where J_d and J_{72} are the moments of inertia of, respectively, the extra disc mounted on the output shaft and the external 72–tooth gear. With the aid of the free–body diagram reported in Fig. 3 (which highlights the internal torques exchanged between the bodies), the following lumped–parameter LTI model of the DC gearmotor can be easily derived:

$$\begin{cases} L_a \dfrac{di_a}{dt} + (R_a + R_s)\, i_a \;=\; u_{drv} - u_e & \text{(electrical dynamics)} \quad (1) \\ J_m \dfrac{d\omega_m}{dt} + B_m\, \omega_m \;=\; \tau_m - \tau'_l & \text{(rotor mechanical dynamics)} \quad (2) \\ J_l \dfrac{d\omega_l}{dt} + B_l\, \omega_l \;=\; \tau_l - \tau_d & \text{(load mechanical dynamics)} \quad (3) \end{cases}$$

with

$$\begin{cases} u_e \;=\; k_e\, \omega_m & \text{(law of generators)} \quad (4) \\ \tau_m \;=\; k_t\, i_a & \text{(law of motors)} \quad (5) \end{cases}$$

and

$$\begin{cases} \omega_l \;=\; \omega_m / N & \text{(gearbox speed transformation)} \quad (6) \\ \tau_l \;=\; N\, \tau'_l & \text{(gearbox torque transformation)} \quad (7) \end{cases}$$

The equation (7) is derived from the power balance of an ideal gearbox with a 100% efficiency, i.e. by assuming that the gearbox mechanical input power $P_m = \tau'_l\, \omega_m$ is equal to the output power $P_l = \tau_l\, \omega_l$. The torque τ_d in (3) represents a generic disturbance torque exerted at the load side. It can be used to model any externally applied torque. In this handout, it is used to account for the *Coulomb* (*static*) friction of the mechanical transmission. The Coulomb friction can be modelled as a constant resistant torque which opposes to the load movement, namely:

$$\tau_d \;=\; \tau_{sf}\, \mathrm{sign}(\omega_l)\,, \qquad \tau_{sf} > 0 \qquad \text{(Coulomb friction at } \textit{load side}\text{)} \quad (8)$$

The overall mechanical dynamics can be obtained by combining (2), (3) with (6), (7); at *motor side*,

it holds that:

$$J_{eq}\,\frac{d\omega_m}{dt} \;+\; B_{eq}\,\omega_m \;=\; \tau_m \;-\; \frac{1}{N}\,\tau_d \qquad \left(\begin{array}{c}\text{overall mechanical dynamics}\\ \text{at } \textit{motor side}\end{array}\right) \tag{9}$$

where

$$J_{eq} \;=\; J_m \;+\; \frac{J_l}{N^2}\,, \qquad B_{eq} \;=\; B_m \;+\; \frac{B_l}{N^2} \tag{10}$$

are the total inertia and viscous friction as "seen" at *motor side*. Alternatively, at *load side*, the overall mechanical dynamics is:

$$N^2\,J_{eq}\,\frac{d\omega_l}{dt} \;+\; N^2\,B_{eq}\,\omega_l \;=\; N\,\tau_m \;-\; \tau_d \qquad \left(\begin{array}{c}\text{overall mechanical dynamics}\\ \text{at } \textit{load side}\end{array}\right) \tag{11}$$

with $N^2\,J_{eq}$ and $N^2\,B_{eq}$ being the total inertia and viscous friction "seen" at *load side*. From (9), note that the total friction torque (viscous + static) generated at the motor side is equal to:

$$\tau'_f \;=\; B_{eq}\,\omega_m \;+\; \frac{\tau_{sf}}{N}\,\mathrm{sign}\,(\omega_m) \qquad (\text{total friction at } \textit{motor side}) \tag{12}$$

At load side, the total friction is equal to:

$$\tau_f \;=\; N\,\tau'_f \;=\; N^2\,B_{eq}\,\omega_l \;+\; \tau_{sf}\,\mathrm{sign}\,(\omega_l) \qquad (\text{total friction at } \textit{load side}) \tag{13}$$

The voltage u_{drv} in (1) is provided by the voltage driver, which is a power operational amplifier (op–amp) with a non–inverting configuration. Therefore, it holds that:

$$u_{drv} \;=\; \left(1 + \frac{R_3}{R_4}\right) u_+ \tag{14}$$

where u_+ is the voltage at the non–inverting input of the op–amp. By noting that the currents flowing through the capacitor C_1 and the resistance R_2 are, respectively, $i_1 = C_1\,du_+/dt$ and $i_2 = u_+/R_2$, so that $u_+ = u - R_1\,(i_1 + i_2)$, it is possible to obtain the following relation between the two voltages u and u_+ (after some algebraic manipulations):

$$\left(\frac{R_1 R_2 C_1}{R_1 + R_2}\right)\frac{du_+}{dt} \;+\; u_+ \;=\; \frac{R_2}{R_1 + R_2}\,u \tag{15}$$

By combining (14) and (15) it finally holds that:

$$\left(\frac{R_1 R_2 C_1}{R_1 + R_2}\right)\frac{du_{drv}}{dt} \;+\; u_{drv} \;=\; \left(1 + \frac{R_3}{R_4}\right)\frac{R_2}{R_1 + R_2}\,u \tag{16}$$

After defining

$$k_{drv} \;=\; \left(1 + \frac{R_3}{R_4}\right)\frac{R_2}{R_1 + R_2}\,, \qquad T_{drv} \;=\; \frac{R_1 R_2 C_1}{R_1 + R_2} \tag{17}$$

the equation (16) can be rewritten as

$$T_{drv}\,\frac{du_{drv}}{dt} \;+\; u_{drv} \;=\; k_{drv}\,u \qquad (\text{voltage driver dynamics}) \tag{18}$$

which resembles the dynamics of a first order low–pass filter with time constant T_{drv} (and hence cut–off frequency $\omega_c = 1/T_{drv}$ in $[\mathrm{rad/s}]$ units, or $f_c = 1/(2\pi T_{drv})$ in $[\mathrm{Hz}]$ units) and DC gain k_{drv}.

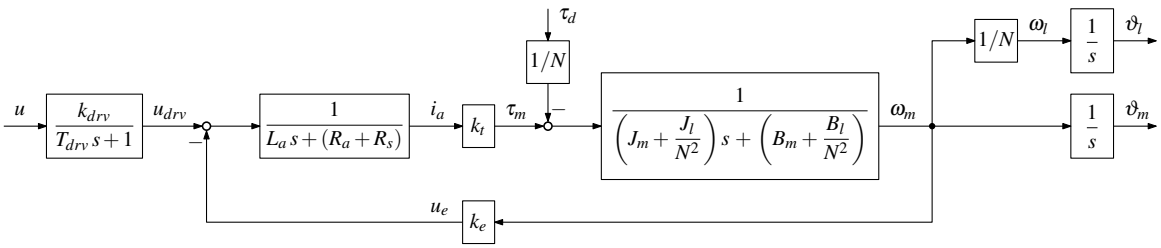

Figure 4: DC gearmotor: block diagram.

After using (4) in (1), (5) in (9) and after recalling (18), the following analytical model of the DC gearmotor with inertial load is finally obtained:

$$\begin{cases} L_a \dfrac{di_a}{dt} + R_{eq}\, i_a = u_{drv} - k_e\, \omega_m & (19) \\ J_{eq} \dfrac{d\omega_m}{dt} + B_{eq}\, \omega_m = k_t\, i_a - \dfrac{1}{N}\, \tau_d & (20) \\ T_{drv} \dfrac{du_{drv}}{dt} + u_{drv} = k_{drv}\, u & (21) \end{cases}$$

where

$$R_{eq} = R_a + R_s \tag{22}$$

By applying the Laplace transform to both sides of (19)–(21), the following set of algebraic equations result:

$$\begin{cases} (L_a\, s + R_{eq})\, I_a(s) = U_{drv}(s) - k_e\, \Omega_m(s) & (23) \\ (J_{eq}\, s + B_{eq})\, \Omega_m(s) = k_t\, I_a(s) - \dfrac{1}{N}\, T_d(s) & (24) \\ (T_{drv}\, s + 1)\, U_{drv}(s) = k_{drv}\, U(s) & (25) \end{cases}$$

which corresponds to the block diagram shown in Fig. 4. After some algebraic manipulations, it follows that:

$$P_{u\to\omega_m}(s) = \frac{\Omega_m(s)}{U(s)} = \frac{k_{drv}}{T_{drv}s+1} \cdot \frac{k_t}{(L_a\, s + R_{eq})(J_{eq}\, s + B_{eq}) + k_t\, k_e} \tag{26}$$

Since $\omega_l = \omega_m/N$ and $\omega_l = d\vartheta_l/dt$, so that $\Theta_l(s) = \Omega_m(s)/(Ns)$, it finally holds that:

$$P_{u\to\vartheta_l}(s) = \frac{\Theta_l(s)}{U(s)} = \frac{k_{drv}}{T_{drv}s+1} \cdot \frac{k_t}{(L_a\, s + R_{eq})(J_{eq}\, s + B_{eq}) + k_t\, k_e} \cdot \frac{1}{Ns} \tag{27}$$

Typically, the time constants of the voltage driver and the armature circuit are both very small, i.e.

$$L_a/R_{eq} \ll 1\,, \qquad T_{drv} \ll 1 \tag{28}$$

so that the transfer function (27) can be simplified as follows:

$$P(s) = \frac{k_{drv}\, k_t}{R_{eq}\,(J_{eq}\, s + B_{eq}) + k_t\, k_e} \cdot \frac{1}{Ns} = \frac{k_m}{T_m\, s\, +\, 1} \cdot \frac{1}{Ns} \tag{29}$$

with

$$k_m = \frac{k_{drv}\, k_t}{R_{eq}\, B_{eq} + k_t\, k_e}\,, \qquad T_m = \frac{R_{eq}\, J_{eq}}{R_{eq}\, B_{eq} + k_t\, k_e} \tag{30}$$

Armature resistance	R_a	$2.6\,\Omega$
Armature inductance	L_a	$180\,\mu\mathrm{H}$
Electric (BEMF) constant	k_e	$7.68 \times 10^{-3}\,\mathrm{Vs/rad}$
Torque constant	k_t	$7.682 \times 10^{-3}\,\mathrm{Nm/A}$
Rotor inertia	J_m	$3.90 \times 10^{-7}\,\mathrm{kg\,m^2}$
Rotor viscous friction coefficient	B_m	not available
Gearbox ratio	N	14
Moment of inertia of external 72–tooth gear	J_{72}	$1.4 \times 10^{-6}\,\mathrm{kg\,m^2}$
Moment of inertia of extra disc	J_d	$3.0 \times 10^{-5}\,\mathrm{kg\,m^2}$
Load viscous friction coefficient	B_l	to be estimated
Voltage driver static gain	k_{drv}	≈ 0.6
Voltage driver cut–off frequency	$f_{c,drv}$	$\approx 1.2\,\mathrm{kHz}$
Shunt resistance	R_s	$0.5\,\Omega$

Table 2: DC gearmotor (plant) nominal parameters.

The nominal values of the plant parameters are reported in Tab. 2 (see also the introductory guide to the experimental setup).

3 PID control design with frequency response methods

3.1 Formulation of control design specifications for the loop transfer function

Control design specifications define the desired characteristics of a control system response. These specifications include:

1) *stability specifications*: the control system must be internally stable in both nominal (*nominal stability*) and perturbed (*robust stability*) cases.

2) *performance specifications*:

- *static performance specifications*: quantify the desired steady state accuracy in tracking the reference input and rejecting external disturbances and noises.
- *dynamic performance specifications*: quantify the quality of the transient response, (typically the speed of response) to both the reference input and external disturbances.

As for the stability specifications, the performance specifications must be usually satisfied in both the nominal (*nominal performance*) and perturbed (*robust performance*) cases.

A design specification can be formulated either in the *time* or *frequency domain*:

- A *time domain specification* imposes a desired value for a "time dependent" quantity, which is typically a parameter of the time response, evaluated in terms of the control error, controlled output or control signal.
- A *frequency domain specification* imposes a desired value for a "frequency dependent" quantity, which is typically a parameter of the sensitivity or complementary sensitivity transfer functions of the feedback control system.

The most typical time domain specifications are:

- for the *static performance specifications*, the maximum control error amplitude that is tolerated at steady state, in response to canonical inputs (e.g. unist step, ramp, parabolic ramp, etc.).
- for the *dynamic performance specifications*, the overshoot (M_p) and the rising (t_r) or settling ($t_{s,1\%}$ and $t_{s,5\%}$ for settling at 1% and 5%, respectively) times of the step response.

The most typical frequency domain specification are:

- for the *static performance specifications*, the gain of the sensitivity or complementary sensitivity functions at low frequencies.
- for the *dynamic performance specifications*, the resonant peak amplitude (M_r) and the closed–loop bandwidth (ω_B).

The rising or settling times in the step response and the closed–loop bandwidth are both measures of the "system promptness" (i.e. they quantify how quickly the system reacts to abrupt changes of its inputs), while the overshoot peak in the step response and the resonant peak in the frequency response are both measures of the "relative stability" (i.e. they quantify how much the system is damped). When the closed–loop system dynamics can be approximated with that of a first or second order system (dominant poles approximation), then some approximated relationships between the time and frequency domain parameters can be given. In particular, when the closed–loop system admits a second order dominant poles approximation of the type

$$T(s) \;=\; \frac{\omega_n^2}{s^2 \,+\, 2\delta\omega_n s \,+\, \omega_n^2}\,, \qquad 0 \leq \delta < 1 \tag{31}$$

then:

- the closed–loop bandwidth is approximatively equal to the frequency of the dominant poles, i.e. $\omega_B \approx \omega_n$.

  Then, by knowing that the typical parameters of the step response of a second order system are related to the damping and natural frequencies of the system poles by the following expressions

$$t_r \;\approx\; \frac{1.8}{\omega_n}\,, \qquad t_{s,5\%} \;=\; \frac{3}{\delta\omega_n}\,, \qquad t_{s,1\%} \;=\; \frac{4.6}{\delta\omega_n} \tag{32}$$

$$M_p \;=\; e^{-\frac{\pi\delta}{\sqrt{1-\delta^2}}} \tag{33}$$

  it follows that

$$\omega_B\, t_r \;\approx\; 1.8 \tag{34}$$

$$\omega_B\, t_{s,5\%} \;\approx\; 3/\delta \qquad \text{and} \qquad \omega_B\, t_{s,1\%} \;\approx\; 4.6/\delta \tag{35}$$

  which relate the closed–loop bandwidth to time–domain specifications such as the rising or settling (with prescribed overshoot) times. The damping factor in (35) is determined from a prescribed overshoot by using the inverse of (33), namely

$$\delta \;=\; \frac{\log(1/M_p)}{\sqrt{\pi^2 + \log^2(1/M_p)}} \tag{36}$$

  The function (36) is plotted in Fig. 5a.

- the overshoot M_p and the resonant peak M_r are such that

$$M_p \;\approx\; \frac{M_r}{|T(j0)|} \;-\; 1 \tag{37}$$

  where $|T(j0)|$ is the static gain of the closed–loop system.

Since the controller dynamics directly affects the loop transfer function $L(s) = C(s)\,P(s)$ of the feedback control system (where $C(s)$ and $P(s)$ are the controller and plant transfer functions, respectively), it is convenient, for the purpose of control design, to translate the control design specifications, formulated either in time or frequency domain, into equivalent specifications for the loop transfer function. It holds that:

- the steady state control error e_{ss} in response to a canonical reference input $r(t)$ depends on the number of poles at the origin (*system type*) and the Bode gain of the loop transfer function. In particular, a static performance specification of the type [1]:
  - $e_{ss} = 0$ with $r(t) = \delta_{-1}(t),\, \delta_{-2}(t),\, \ldots, \delta_{-h}(t)$
  - $|e_{ss}| \leq \varepsilon$ with $r(t) = \delta_{-(h+1)}(t)$

  imposes the following structure for the loop transfer function:

$$L(s) \;=\; \frac{K_l}{s^h}\,\hat{L}(s) \qquad \text{with} \qquad \hat{L}(0) = 1 \quad \text{and} \quad K_l \geq 1/\varepsilon \tag{38}$$

- for a closed–loop system that admits a second order dominant pole approximation as (31), the closed–loop bandwidth and the gain crossover frequency ω_{gc} (i.e. frequency where the loop transfer function has unit magnitude, $|L(j\omega_{gc})| = 1$) are approximately equal. Therefore, from (34) and (35) it follows that

$$\omega_{gc} \;\approx\; \frac{1.8}{t_r} \tag{39}$$

  and

$$\omega_{gc} \;\approx\; \frac{3}{\delta\, t_{s,5\%}} \qquad \text{and} \qquad \omega_{gc} \;\approx\; \frac{4.6}{\delta\, t_{s,1\%}} \tag{40}$$

- for a closed–loop system that admits a second order dominant pole approximation as (31), the phase margin φ_m (i.e. the quantity $\varphi_m = -\pi + \angle\, L(j\omega_{gc})$) and the damping factor δ are related by the expression

$$\varphi_m \;=\; \operatorname{atan} \frac{2\delta}{\sqrt{\sqrt{1 + 4\delta^4} - 2\delta^2}} \tag{41}$$

  The damping factor in (41) is determined from a prescribed overshoot by using (36). By combining the two expressions, the plot of Fig. 5b is obtained. Note that for phase margins below 70°, the approximation $\delta \approx \varphi_m/100$ is valid.

Once the specifications for the loop transfer function have been formulated, the controller design can be conveniently carried out with the Bode's method (frequency response method).

[1] $\delta_{-1}(t)$ denotes the unit step signal; $\delta_{-h}(t) = t^{h-1}\delta_{-1}(t)$ is the h–th causal polynomial signal (e.g. linear ramp, parabolic ramp, etc).

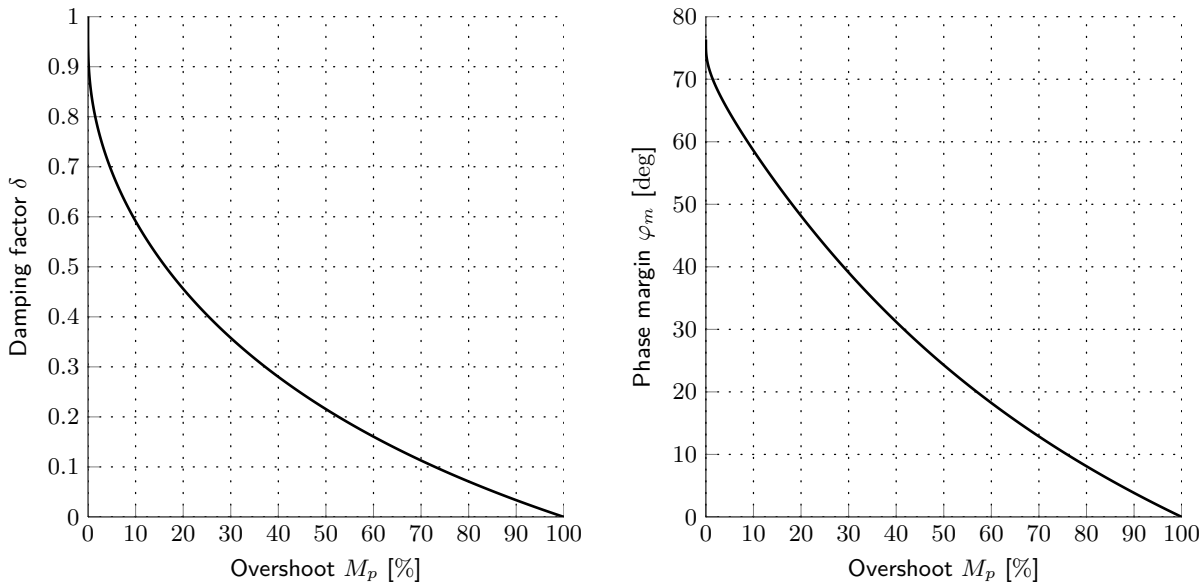

(a) (b)

Figure 5: (a) Damping factor vs overshoot – see (36); (b) Phase margin vs overshoot – see (41).

3.2 PID controller design with the Bode's method

In its general formulation, the Bode's method for the synthesis of a controller $C(s)$ consists of adding basic dynamic compensators (lead/lag networks) $C_i(s)$ in series to the plant $P(s)$ till the resulting loop transfer function $L(s) = \prod_i C_i(s)\, P(s)$ satisfies the design specifications, translated into properties of the open-loop transfer functions as the phase and gain margin.
In this laboratory activity, the controller structure is selected a priori to be that of a PID controller

$$C(s) \;=\; K_P \,+\, \frac{K_I}{s} \,+\, K_D\, s \;=\; K_P \left(1 \,+\, \frac{1}{T_I s} \,+\, T_D\, s\right) \tag{42}$$

and the Bode's method is only applied to determine the values of the controller parameters K_P, K_I and K_D (or K_P, T_I and T_D) that meet the design requirements on the gain crossover frequency ω_{gc} and phase margin φ_m, i.e. to have

$$L(j\omega_{gc}) \;=\; C(j\omega_{gc})\, P(j\omega_{gc}) \;=\; e^{j(-\pi+\varphi_m)} \tag{43}$$

From (43) it follows that

$$C(j\omega_{gc}) \;=\; \Delta K\, e^{\Delta\varphi} \qquad \text{with} \qquad \Delta K = |P(j\omega_{gc})|^{-1}, \quad \Delta\varphi = -\pi + \varphi_m - \angle P(j\omega_{gc}) \tag{44}$$

By combining (44) with (42), and equating the real and imaginary parts at the two sides of the identity, it holds that

$$\begin{cases} K_P \;=\; \Delta K\, \cos\Delta\varphi & (45) \\ \omega_{gc}\, T_D \,-\, \dfrac{1}{\omega_{gc}\, T_I} \;=\; \tan\Delta\varphi & (46) \end{cases}$$

To solve the underdetermined system of two equations (45) and (46) in the three unknowns K_P, T_I and T_D, the extra constraint

$$T_I \;=\; \alpha\, T_D \quad \text{with} \quad \alpha \geq 4 \tag{47}$$

is generally introduced, so that finally

$$\begin{cases} K_P &= \Delta K \cos \Delta\varphi & (48) \\ T_D &= \dfrac{\tan \Delta\varphi + \sqrt{(\tan(\Delta\varphi))^2 + 4/\alpha}}{2\,\omega_{gc}} & (49) \\ T_I &= \alpha T_D & (50) \end{cases}$$

Moreover, $K_D = K_P T_D$ and $K_I = K_P / T_I$. Note that:

1. for the design of a PI or a PD controller, the condition (44) directly provides the values of the controller gains, with no need to introduce extra constraints such as (47). In fact, for a PI or PD controller it follows that:

$$\begin{cases} K_P &= \Delta K \cos \Delta\varphi \\ K_D &= \dfrac{1}{\omega_{gc}} \Delta K \sin \Delta\varphi \end{cases} \qquad \text{(PD controller)} \qquad (51)$$

$$\begin{cases} K_P &= \Delta K \cos \Delta\varphi \\ K_I &= -\omega_{gc} \Delta K \sin \Delta\varphi \end{cases} \qquad \text{(PI controller)} \qquad (52)$$

2. The ideal derivative in (42) is not physically implementable. It is usually replaced with a high–pass filter ("real derivative") that approximates the frequency response of the ideal derivative in the low frequency range. A typical choice is

$$H(s) = \frac{s}{T_L s + 1} \qquad (53)$$

where T_L is chosen to get a satisfactory rejection of the measurement noise outside of the control bandwidth: typically, the parameter is set so that the filter cut–off frequency $1/T_L$ is $2 \div 5$ times larger of the gain crossover frequency ω_{gc}.

After the synthesis, the internal stability of the control system can verified by using the results that have been presented in class, and the design adjusted if needed by modifying the desired phase margin.

4 Estimation of model parameters

In principle, the control design can be carried out on a nominal model of the plant, provided that a sufficiently large phase margin is selected for tolerating possible parameter uncertainties that could potentially destabilise the control system. However, better performances can be usually achieved when the actual values of the plant parameters are estimated from the experimental data. In this section it is described a simple experimental procedure for the estimation of the main mechanical parameters, such as the friction (static and viscous) and the total rotor inertia. These parameters can be used to improve the control design, either by redesigning the feedback controller with the updated model plant, or by implementing a feedforward compensator through which better tracking performance can be achieved.

4.1 Friction estimation

Reconsider the overall mechanical dynamics at motor side reported in (9). After rearranging the terms, the following torque balance equation results

$$\tau_m \;=\; J_{eq}\,\frac{d\omega_m}{dt} \;+\; B_{eq}\,\omega_m \;+\; \frac{1}{N}\,\tau_d \tag{54}$$

which shows that at any instant, a fraction of the motor torque τ_m, namely the *inertial torque* component

$$\tau_i \;\triangleq\; J_{eq}\,\frac{d\omega_m}{dt} \tag{55}$$

is used to accelerate the equivalent rotor inertia J_{eq}, while the remaining part is required to overcome the *total friction torque*:

$$\tau_f' \;=\; B_{eq}\,\omega_m \;+\; \frac{1}{N}\,\tau_d \qquad \text{(total friction at } \textit{motor side}\text{)} \tag{56}$$

Note that the total friction torque consists of two terms, namely the *viscous friction torque* component $B_{eq}\,\omega_m$, and the *static (or Coulomb) friction* component τ_d/N (as seen at motor side), with τ_d as defined in (8). Suppose that the motor is operating at steady state with *constant speed*, i.e. $d\omega_m/dt = 0$; then from the torque balance equation (54), it follows that

$$\tau_m \;=\; \tau_f' \;=\; B_{eq}\,\omega_m \;+\; \frac{\tau_{sf}}{N}\,\mathrm{sign}(\omega_m) \qquad \text{with} \qquad \frac{d\omega_m}{dt} = 0 \tag{57}$$

which shows that for keeping the motor running at constant speed, the motor torque τ_m has to exactly balance the friction torque τ_f'. This torque balance can be effectively exploited to estimate the two friction parameters B_{eq} and τ_{sf} in (57), as shown in the remaining part of this section. In fact, suppose to measure the motor torque at different *constant* speed levels. A direct measurement of the motor torque is obviously not possible with the available experimental setup (a torque meter is required for the purpose); however, the law of motor (5) shows that an indirect measurement is possible by sensing the motor current i_a, provided that the torque constant K_t is known. In the experimental setup, remind that the armature current can be indirectly measured by sensing the voltage drop across the shunt resistor R_s. Once the torque is known, the viscous and static friction coefficients in the affine function (57) can be estimated by performing a conventional linear least squares (LS) fitting of the torque vs speed data. For such purpose, rewrite the model (57) in *linear*

regression form as follows:

$$\tau_m \;=\; \tau'_f \;=\; \boldsymbol{\varphi}^T\,\boldsymbol{\theta} \tag{58}$$

where

$$\boldsymbol{\varphi}^T \;=\; \Big[\omega_m\,,\quad (1/N)\,\mathrm{sign}(\omega_m)\Big]\,,\qquad \boldsymbol{\theta} \;=\; \Big[B_{eq}\,,\quad \tau_{sf}\Big]^T \tag{59}$$

are, respectively, the vectors of *regressors* and *unknown parameters* to be estimated. Let

$$Z^M \;=\; \{\tau_{m,k},\;\; \omega_{m,k}\} \qquad \text{with} \quad k \,=\, 0,\,\ldots,\,M-1 \tag{60}$$

denote the set of torque/speed pairs measured at M different constant speed levels. The vector of unknown parameters $\boldsymbol{\theta}$ can be determined by minimising the quadratic cost function (quadratic error)

$$V(\boldsymbol{\theta}) \;=\; \sum_{k=0}^{M-1} \Big(\tau_{m,k} \,-\, \boldsymbol{\varphi}_k^T\,\boldsymbol{\theta}\Big)^2 \tag{61}$$

where

$$\boldsymbol{\varphi}_k^T \;=\; \Big[\omega_{m,k}\,,\quad (1/N)\,\mathrm{sign}(\omega_{m,k})\Big] \tag{62}$$

With the notation

$$\boldsymbol{Y} \;=\; \begin{bmatrix} \tau_{m,0} \\ \tau_{m,1} \\ \vdots \\ \tau_{m,M-1} \end{bmatrix} \in \mathbb{R}^{M\times 1}\,,\qquad \boldsymbol{\Phi} \;=\; \begin{bmatrix} \boldsymbol{\varphi}_0^T \\ \boldsymbol{\varphi}_1^T \\ \vdots \\ \boldsymbol{\varphi}_{M-1}^T \end{bmatrix} \in \mathbb{R}^{M\times 2} \tag{63}$$

the cost function can be rewritten as

$$V(\boldsymbol{\theta}) \;=\; [\boldsymbol{Y} - \boldsymbol{\Phi}\,\boldsymbol{\theta}]^T\,[\boldsymbol{Y} - \boldsymbol{\Phi}\,\boldsymbol{\theta}] \tag{64}$$

which is minimised by the least squares (LS) solution

$$\hat{\boldsymbol{\theta}}_{LS} \;=\; \Big[\hat{B}_{eq}\,,\quad \hat{\tau}_{sf}\Big]^T \;=\; \Big(\boldsymbol{\Phi}^T\boldsymbol{\Phi}\Big)^{-1}\,\boldsymbol{\Phi}^T\,\boldsymbol{Y} \tag{65}$$

The LS estimate $\hat{\tau}'_f$ of the total friction torque is therefore

$$\hat{\tau}'_f \;=\; \hat{B}_{eq}\,\omega_m \,+\, \frac{\hat{\tau}_{sf}}{N}\,\mathrm{sign}(\omega_m) \tag{66}$$

Note: in Matlab, suppose to have defined the matrices $\boldsymbol{\Phi}$ and $\boldsymbol{Y}$ with variables names `Phi` and `Y`; then, the least squares solution (65) can be computed by using the *left matrix division* operator "\", i.e. `thLS = Phi\Y` (consult `mldivide` on the online help).

4.2 Inertia estimation

Suppose to impose a constant acceleration/deceleration to the total gearmotor inertia, i.e. to increase/decrease the motor speed at a constant rate. From (54)–(56) it follows that an estimate $\hat{\tau}_i$ of the inertial torque component τ_i used to accelerate/decelerate the equivalent inertia can be obtained by subtracting from the measured motor torque τ_m the friction torque $\hat{\tau}'_f$ estimated with

the procedure outlined in the previous Sec. 4.1, namely

$$\hat{\tau}_i \;=\; \tau_m \;-\; \hat{\tau}'_f \;=\; \hat{J}_{eq}\,\frac{d\omega_m}{dt} \qquad \text{with} \qquad \frac{d\omega_m}{dt} \;\neq\; 0 \tag{67}$$

Let $\hat{\tau}_{i+} > 0$ be the average inertial torque estimated with constant acceleration $a_{m+} = d\omega_m/dt > 0$; similarly, let $\hat{\tau}_{i-} < 0$ be the average inertial torque estimated with constant deceleration $a_{m-} = d\omega_m/dt < 0$. Then, the total rotor inertia can be estimated as follows

$$\hat{J}_{eq} \;=\; \frac{\hat{\tau}_{i+} \;-\; \hat{\tau}_{i-}}{a_{m+} \;-\; a_{m-}} \tag{68}$$

If multiple acceleration/deceleration phases are repeated over time, then the estimate of the total rotor inertia can be obtained by averaging the single inertia estimates obtained for each acceleration/deceleration phase, i.e.

$$\hat{J}_{eq} \;=\; \frac{1}{M}\,\sum_{n=1}^{M}\,\hat{J}_{eq,n} \tag{69}$$

where $\hat{J}_{eq,n}$ is the inertia estimate obtained for the n^{th} acceleration/deceleration phase (using (68)), namely

$$\hat{J}_{eq,n} \;=\; \frac{\hat{\tau}_{i+,n} \;-\; \hat{\tau}_{i-,n}}{a_{m+,n} \;-\; a_{m-,n}} \tag{70}$$

and M denotes the total number of phases.

4.3 Alternative approach: *combined* friction and inertia estimation

A single experimental test can be used as a replacement of the previous two tests for the simultaneous estimation of the friction and inertia parameters. Rewrite the torque balance (54) in linear regression form

$$\tau_m \;=\; \boldsymbol{\varphi}^T\,\boldsymbol{\theta} \tag{71}$$

where

$$\boldsymbol{\varphi}^T \;=\; \left[\frac{d\omega_m}{dt}\,,\quad \omega_m\,,\quad (1/N)\,\mathrm{sign}(\omega_m)\right]\,, \qquad \boldsymbol{\theta} \;=\; [J_{eq},\quad B_{eq},\quad \tau_{sf}]^T \tag{72}$$

are, respectively, the vectors of regressors and unknown parameters to be estimated. The estimation problem can be formulated as follows: with the availability of the experimental data (measurements)

$$Z^M = \{\tau_m(t_k),\;\; \omega_m(t_k)\} \qquad \text{with} \qquad t_k = k\,T_s\,,\quad k = 0,\,\ldots,\,M-1 \tag{73}$$

determine the vector of parameters $\boldsymbol{\theta}$ that minimises the quadratic cost function (quadratic error)

$$J \;=\; \sum_{k=0}^{M-1}\,\Big[\tau_m(t_k) \;-\; \boldsymbol{\varphi}^T(t_k)\,\boldsymbol{\theta}\Big]^2 \tag{74}$$

With the notation

$$\boldsymbol{Y} \;=\; \begin{bmatrix} \tau_m(t_0) \\ \tau_m(t_1) \\ \vdots \\ \tau_m(t_{M-1}) \end{bmatrix} \in \mathbb{R}^{M\times 1}\,, \qquad \boldsymbol{\Phi} \;=\; \begin{bmatrix} \boldsymbol{\varphi}^T(t_0) \\ \boldsymbol{\varphi}^T(t_1) \\ \vdots \\ \boldsymbol{\varphi}^T(t_{M-1}) \end{bmatrix} \in \mathbb{R}^{M\times 3} \tag{75}$$

the cost function can be rewritten as in (64), which is then minimised by the LS solution

$$\hat{\boldsymbol{\theta}}_{LS} \;=\; \left[\hat{J}_{eq}\,,\quad \hat{B}_{eq}\,,\quad \hat{\tau}_{sf}\right] \tag{76}$$

which is computed by using the expression (65). For the identifiability of the model parameters, the data (73) must be collected under sufficient *excitation conditions* of the plant dynamics. For such purpose, it is sufficient to impose constant acceleration/deceleration phases to the motor during the data collection experiment.